

We are IntechOpen, the world's leading publisher of Open Access books Built by scientists, for scientists

6,900

Open access books available

186,000

International authors and editors

200M

Downloads

Our authors are among the

154

Countries delivered to

TOP 1%

most cited scientists

12.2%

Contributors from top 500 universities



WEB OF SCIENCE™

Selection of our books indexed in the Book Citation Index
in Web of Science™ Core Collection (BKCI)

Interested in publishing with us?
Contact book.department@intechopen.com

Numbers displayed above are based on latest data collected.
For more information visit www.intechopen.com



Influence of Gamma Radiation on Gas-Filled Surge Arresters

Luka Rubinjoni, Katarina Karadžić and Boris Lončar

Abstract

Current knowledge on the impact of γ radiation on gas-filled surge arresters (GFSA) is presented. Miniaturization of electronic components has led to their increased vulnerability to overvoltage. The combination of ionizing radiation and voltage surges is present in both space exploration and military applications. Some of the commonly used overvoltage protection components (transient suppressor diodes and metal-oxide varistors) perform poorly under ionizing radiation. GFSA demonstrate improved performance under γ irradiation. Performance of GFSA was tested under neutron + γ radiation, considering the effects of induced radiation. The effects of γ radiation were tested on commercially available GFSA components and on the purpose-built GFSA model. The model was used to measure the prebreakdown current and breakdown voltage of different electrode materials (aluminum, steel, brass) under varying gas pressures, under DC and pulse currents. The improvement of the performance of GFSA due to external γ radiation, combined with other improvements in the design (hollow cathode), can enable the use of GFSA without internal radiation sources in environments where γ radiation is present.

Keywords: overvoltage protection, gamma radiation, electromagnetic pulse, power surge, gas-filled surge arrestor

1. Introduction

The advances in complexity and continuous miniaturization of electronic components make them increasingly vulnerable to damage caused by overvoltage events. Modern integrated circuits may suffer temporary or permanent faults even from small overvoltage, due to the size of the internal components in the nanometer range [1, 2]. Overvoltage transients occur in both power and signal lines, due to natural events like lightning strike, normal operation of electric and electronic devices (commutation, powering the devices on or off), failure of equipment or network connections, electrostatic discharge, or the interaction of device/network conductors and electromagnetic fields. Proper design of circuitry protection is essential in preventing temporary or permanent malfunction caused by surge. The combined effects of fast electromagnetic pulse and ionizing radiation present a special challenge to the resilience of electronic components [3].

Depending on their principle of operation and response to voltage transients, overvoltage components can be linear and nonlinear. Linear overvoltage protection components are systems of coils and capacitors assembled into filters of different types. Nonlinear overvoltage protection components come into effect upon the

voltage reaching a certain threshold. Commonly used are transient suppression diodes (TSD), metal-oxide varistors (MOV), and gas-filled surge arresters (GFSA) [4]. The advantages of GFSA compared to the other overvoltage components protection are (1) the ability to conduct high currents (up to 5000 A), (2) low intrinsic capacity (~ 1 pF), and (3) low costs [5]. The disadvantages of GFSA are (1) practical irreversibility of characteristics after the electric arc effect, (2) delayed response, and (3) unsuitability with respect to environmental protection (if GFSA have a radioactive filling) [6–8].

2. Gas-filled surge arresters (GFSA)

The basic design of gas-filled surge arresters is a simple configuration of two or three electrodes encased in a glass or ceramic enclosure filled with insulating gas (**Figure 1**) [9]. The common insulation medium of choice is noble gases [10]. The form of the electrodes is such that it provides a pseudo-homogeneous macro component of the electric field [11]. The strength of the electric field impacts the ratio of free electron generation and loss in the insulating gas. If the field is strong enough, a self-sustained avalanche process will lead to the electrical breakdown of the gas and discharge of the overvoltage [12, 13]. The performance of GFSA is best described by its pulse shape characteristic. The narrower the pulse characteristic is, and the smaller the slope is, the better protective characteristics of GFSA are [6, 7].

Solutions to improve the performance of GFSA in response time include the use of hollow cathodes, thus avoiding radioactive materials or implementing internal radioactive sources [14, 15]. The differences in regulations and standards and the lack of clear strategy for their clear storage and disposal make radioactive sources a challenging solution in the context of radiation protection and potential environmental contamination. Still, there are some natural (cosmic radiation, solar flares, coronal mass ejection) and man-made phenomena (nuclear explosions, especially at high altitude) where the power grid, electrical machinery, and electronic components can experience voltage transients under ionizing radiation.

In order to describe the electrical breakdown of the insulating gas, avalanche coefficients are used to specify the elementary processes in GFSA's gas. Avalanche coefficients that are most commonly used are α , the number of electronic ionization collisions per cm of a distance in the direction of the electric field; η , the number of electrons per cm of a distance in the direction of the field attached to the electrically negative atoms or molecules; and γ , the number of electrons generated

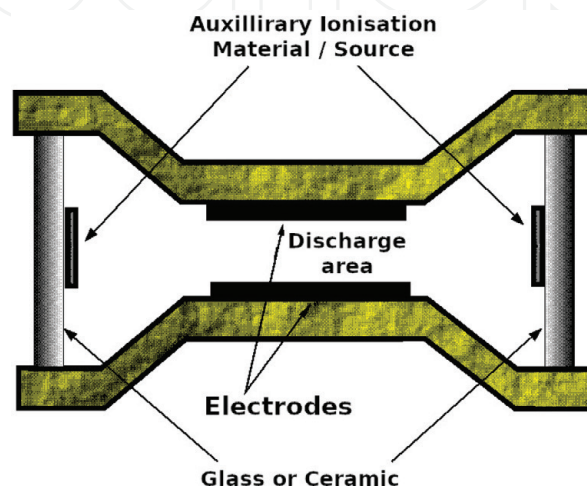


Figure 1.
Schematic of a gas-filled surge arrester [9].

from secondary processes per primary avalanches. The avalanche coefficients vary with pressure and electric field and are not constant for any particular gas or a gas mixture. This dependence has been experimentally determined for most insulating gases and is described as a range of values of the pd product, where p is the insulator gas pressure and d is the distance between the electrodes [1, 11, 16].

The electrical breakdown in gases can be dynamic or static, not depending on the precise mechanism of the electrical breakdown. In gases, static breakdown develops when the rate of voltage variation is significantly lower than the rate of elementary processes occurring during the electrical breakdown of the gas. The breakdown becomes dynamic in the moment these rates become comparable. Depending on the localization of the dominant secondary processes in the system, the static breakdown occurs through the Townsend mechanism or the streamer mechanism. Static breakdown voltage is a deterministic feature of the system, unlike dynamic breakdown that is a stochastic process occurring in a range of voltages [17].

Townsend mechanism is the main pathway of direct current (DC) breakdown, if the secondary processes on the electrodes (e.g., the ionic discharge, photoemission, metastable discharge, etc.) are more prevalent than the secondary processes in the gas (the ionization by positive ions, photo ionization, metastable ionization, etc.) [3]. The value of DC breakdown voltage by Townsend mechanism is described by the following equation:

$$\gamma \int_0^d e^{\int_0^x (\alpha - \eta) dx} \alpha dx = 1 \quad (1)$$

where α is the number of ionization collisions per cm along the electric field, η is the number of electrons per cm along the field associated to electrically negative atoms or molecules, and γ is the number of electrons generated from secondary processes per primary avalanche.

When the secondary processes in the gas are more prevalent than the secondary processes on the electrodes, DC breakdown will occur as streamers, and the breakdown voltage will be dictated by the streamer mechanism [18, 19]. The value of a DC voltage for streamer mechanism breakdown is described by the following equation:

$$\int_0^d [\alpha(x) - \eta(x)] \cdot dx \geq k \quad (2)$$

To describe, determine, and compare the pulse shape characteristics of GFSA, an analytical algorithm has been developed. This approach allows a fast and accurate determination of the GFSA characteristics, without including the irreversible processes resulting from the repeated measurements of the “pulse breakdown voltage” random variable, using different shapes of rapid voltage changes. A pulse shape characteristic (volt-second) represents the breakdown voltage of the GFSA electrode configuration as a function of the applied voltage pulse duration. A decrease in the duration of the pulse results in the increase of the breakdown voltage. Determining the exact pulse characteristic experimentally would require a large number of tests with differently shaped voltage pulses. The application of the area law allows the determination of the pulse shape characteristic based on a single set of measurements using a single pulse voltage shape. The basic assumption in the area law is that plasma-spreading rate in the inter-electrode gap increases linearly due to the rise of the electric field:

$$V(x, t) = k \quad (3)$$

where k is the parameter that depends on electrical discharge mechanism and electrode polarization and E_s is the electric field value corresponding to the DC breakdown voltage U_s . The voltage pulse breakdown condition is given by $u(t) > U_s$, given that the DC breakdown voltage U_s represents the lowest possible value of the breakdown voltage for a specific electrode configuration. Without taking the charge spreading in the inter-electrode gap into account, the following stands:

$$E(x, t) = u(t) \cdot g(x) \quad (4)$$

where $g(x)$ is a function that is to be determined from the specific electrode configuration.

If the complete breakdown occurs through the Townsend mechanism (i.e., k is assumed to be constant along the inter-electrode gap), then according to expressions (3) and (4)

$$\frac{1}{k} \int_{t_1}^{t_1+t_a} \frac{dx}{g(x)} = \int_{t_1}^{t_1+t_a} [u(t) - U_s] dt = P = \text{const} \quad (5)$$

where $x = x_k$ indicates the zone where breakdown through Townsend mechanism changes into breakdown by a streamer, in the moment $t = t_1 + t_a$. In order for a breakdown to occur, a constant surface has to be formed in the voltage-time plane between $u(t)$ and U_s . Thus, measuring the surface P and the DC breakdown voltage U_s is sufficient to determine the pulse shape and pulse breakdown voltage, given that these characteristics of the system do not depend on the applied voltage [7].

A semiempirical method to determine the pulse shape characteristic is performed in the following way: a sequence of DC breakdown voltages is measured (with at least 20 measurements), followed by a sequence of pulse breakdown voltage measurements, by applying the pulse voltage of a stable and defined shape (at least 50 measurements). The corresponding distribution function is obtained by statistical analysis of the measured values. Distribution function allows the determination of the quantities of pulse shape characteristics U_x and U_y desired boundaries (most frequently one takes $x = 0.1\%$ and $y = 99.9\%$). When the mean value of DC breakdown voltage U_s is known, and the quantities are determined, following system of equations can be solved:

$$\begin{aligned} u(t) &= U_s, t = t_1 \\ u(t) &= U_x, t = t_{ax} \\ u(t) &= U_y, t = t_{ay} \end{aligned} \quad (6)$$

Values t_1 , t_{ax} , and t_{ay} allow the determination of surfaces P_x and P_y by applying the area law:

$$\begin{aligned} P_x &= \int_{t_1}^{t_1+t_{ax}} [u(t) - U_s] dt = \text{const} \\ P_y &= \int_{t_1}^{t_1+t_{ay}} [u(t) - U_s] dt = \text{const} \end{aligned} \quad (7)$$

Upon the determination of surfaces P_x and P_y , it is possible to calculate the x th and y th values of the “pulse breakdown voltage” random variable (by applying the area law) for any form of pulse voltage $u(t)$. If the form of pulse voltage is taken as a parameter (in the time interval considered), it is possible to determine x th and y th pulse shape characteristics [7].

3. Radiation resistance of gas-filled surge arresters

The radiation resistance of gas-filled surge arresters (GFSA) is of great importance, especially if the devices are applied in operating regimes with constant, occasional, or potential exposure to ionizing radiation. Natural or artificial atmospheric electromagnetic pulses can cause varying levels of damage to electronic components. Thus, GFSA are very important overvoltage protection components for low-voltage applications in both the military industry and space exploration technologies. Testing of GFSA in comparison to other nonlinear surge arresters has indicated the feasibility of replacing commonly used semiconductor overvoltage components (transient suppressor diodes, metal-oxide varistor), whose protective characteristics significantly degrade when subjected to the radiation [4, 6].

4. Induced radiation effects on GFSA characteristics

In order to test the performance of GFSA under the influence of $n + \gamma$ radiation, the following variables were determined in a $n + \gamma$ field: (1) the random variable “pulse breakdown voltage,” (2) the random variable “DC breakdown voltage,” and (3) the volt-second characteristic. The $n + \gamma$ source was californium isotope ^{252}Cf . This source was selected due to its neutron spectrum resemblance of a nuclear blast’s neutron spectrum [20]. Since the nuclear cross section for capturing a neutron is large enough only for thermal and slow neutron capture and due to the structure of californium source fission spectrum, a relatively small part of neutrons takes part in the neutron activation of GFSA materials. GFSA was subjected to two neutron fluencies: 5.41×10^9 and 16.24×10^{11} n/cm^2 . Along with the neutron component, emitted radiation also has a γ component. The latter influences the electric characteristics of GFSA only for the duration of the exposure to the radiation field. Also, the inelastic interaction cross section of the neutron component is larger than the corresponding γ component cross section [21]. This allows the observation of the effects of radiation resulting from the neutron fluency only. In the experiment, the type and pressure of gas varied in order to get a detailed insight into how the radiation influences the GFSA characteristics.

By measuring 1000 values, the influence on the “DC breakdown voltage” and “pulse breakdown voltage” random variables was tested. During the measurement series, discharge energy (current) was maintained constant. Results of the breakdown voltage obtained in the measurement series were divided into 10 groups of 50 successive values. Statistical tests were performed on each group of results by graphical visualization and chi-squared and Kolmogorov-Smirnov tests. Within each group of measurements, the measured values of breakdown voltage were tested with respect to the type of theoretical distributions (normal, exponential, double exponential, and Weibull’s). U test was used to determine the groups of measurement series having the same random variable (with significance level $\alpha = 5\%$) [17, 22]. The area law was used to explore the effects on the pulse shape (volt-second) characteristic.

The experiments show that the standard deviation of the static breakdown voltage significantly decreased after the irradiation of the GFSA. The pulse voltage tests show that an irradiated GFSA reacts more readily and has somewhat narrower volt-second characteristic than unirradiated GFSA. Effectively, irradiation has improved GFSA’s protective traits. GFSA DC breakdown voltage versus neutron fluency is presented in **Figure 2**. The GFSA volt-second characteristics before and after exposure to the radioactive source, respectively, is presented in **Figure 3A** and **B**.

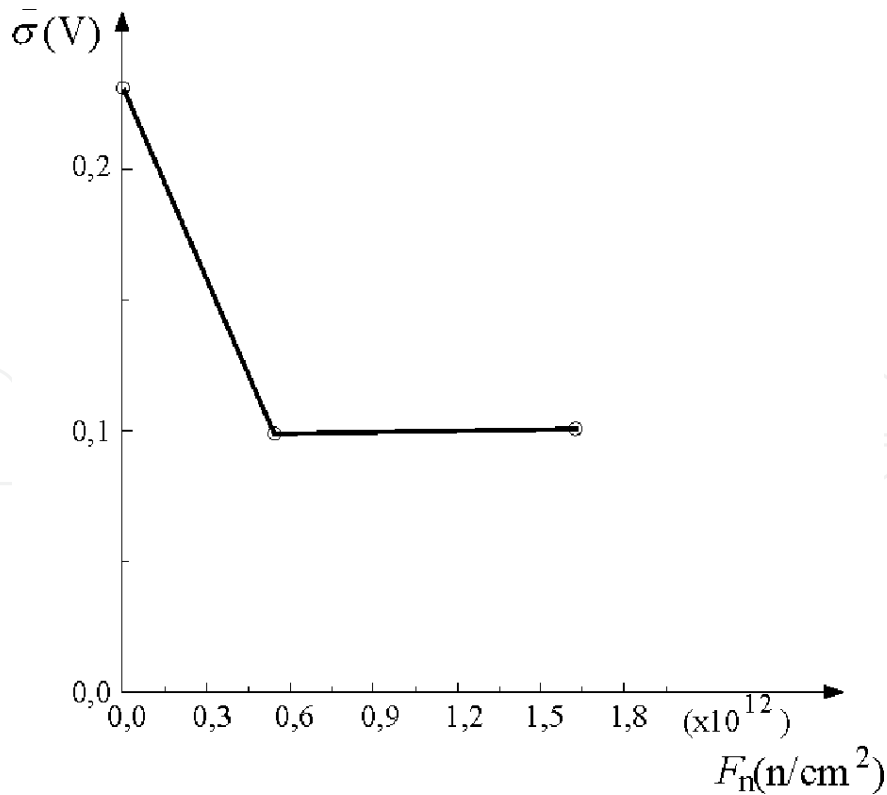


Figure 2.
The GFSA DC breakdown voltage versus neutron fluency characteristic [7].

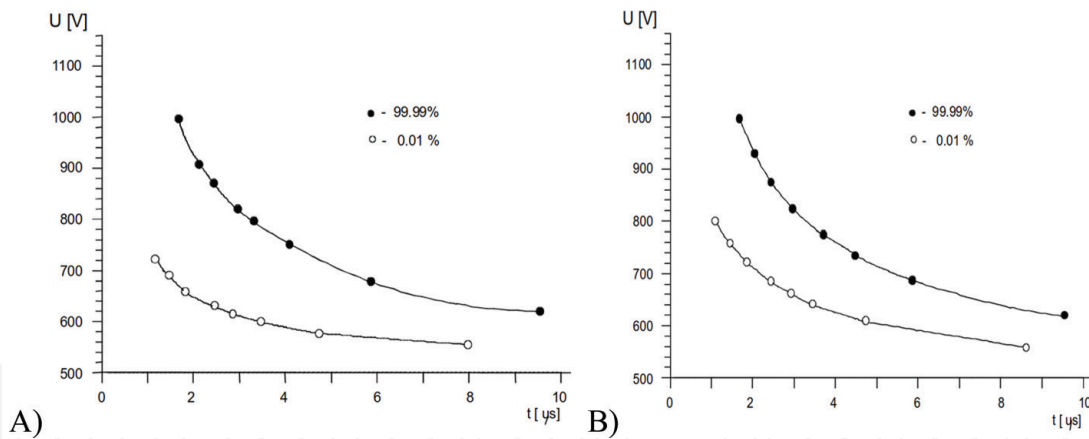


Figure 3.
The GFSA volt-second characteristic before (A) and after (B) radiation [7].

Elevated concentration of free electrons in the inter-electrode gap, resulting from the ionization of the insulating gas, has enabled a faster response of an irradiated GFSA. This ionization was induced by radiation of the GFSA material as a consequence of neutron activation.

GFSA activation analysis diagrams before and immediately after the exposure to the radioactive source, respectively, are presented in **Figure 4A** and **B**. The radioactive isotopes are identified and recorded close to the expected energy peaks. The activity of these isotopes consists of both γ and β component. This induced radioactivity ionizes the gas, leading to the reduction the stochastic dissipation of a pulse breakdown voltage random variable. The improvement to the pulse shape characteristic due to neutron radiation is short lasting, disappearing quickly as the half-lives of induced activities vary from several hours to mere minutes. A diagram of the activation

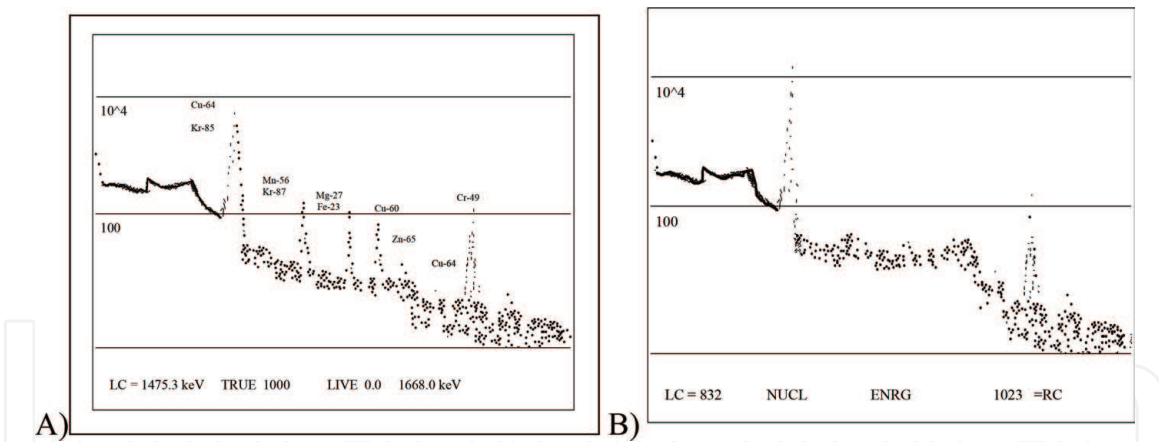


Figure 4. Diagram of the GFSA activation analysis immediately (A) and 6 hours (B) after irradiation [7].

analysis of irradiated GFSA that is taken 6 hours after radiation clearly confirms this effect (**Figure 4B**). In that time frame, most of the active isotopes have degraded to trivial activities, and the GFSA characteristics have returned to unirradiated state.

5. Radiation resistance of commercial GFSA components

An external γ ray source was used to test commercially available GFSA components to analyze the effect of γ radiation. The examination was carried out on the following commercial components (1) SIEMENS (type A) gas surge arresters (nominal voltage 230 V), (2) CITEL BB (type B) bipolar ceramic gas surge arresters (DC spark overvoltage 230 V). The outer dimensions and shape of all components of the same type were the same. The effects of γ radiation on following GFSA characteristics were examined:

1. Prebreakdown current as function of applied voltage
2. Resistance as function of applied voltage

The scheme of the test cycle for investigating the radioactive resistance of GFSA by a DC voltage is depicted in **Figure 5**.

Examination of GFSA radioactive resistance was carried out in a gamma radiation field of ^{60}Co at the Institute of Nuclear Sciences “Vinča.” The average energy of the applied gamma quantum was 1.25 MeV. The dose rate in air was 87.5, 875, and 1750 cGy/h, respectively. The distance between the radioactive source and the examined overvoltage components was 272, 86, and 60 cm, respectively. All tests were performed at room temperature, 20°C.

Test specimens, consisting of 50 commercial components of a single manufacturer, having identical characteristics, have been used in the experiment. During the formation of experimental groups consisting of 50 components each, the nominal characteristics of the tested components have been measured. When the measured values for a particular component exhibited significant discrepancy with respect to the declared values, they were excluded from further testing in accordance to the Sovene’s criterion [2, 8].

The GFSA prebreakdown current as a function of applied voltage without radiation and with γ radiation is shown in **Figure 6A** and **B**, respectively. The diagrams demonstrate:

1. Before the breakdown in the absence of radiation, the current conducted by GFSA is constant and in the order of 0.1 nA. Upon the breakdown, the current rises very sharply (breakdown voltage being 212 V for type A components and 223 V for type B components). When voltage reaches the breakdown level, an abrupt increase of the current takes place, and current values reach μA level. Radiation causes increased numbers of electron-ion pairs in the area between electrodes, leading to the increase of prebreakdown current (consisting of the free electrons and ions reaching electrodes per unit of time). In the moment of breakdown (when one of the free electrons generated in this way becomes initial), an avalanche process generates a breakdown current, the magnitude of which is independent of the prebreakdown current. Ohm's law cannot be applied in this region, given that the observed two-electrode system saturated: all electron-ion pairs generated reach the electrodes in the observed time frame.
2. The influence of γ radiation on GFSA performance is significant. The pre-breakdown current is 10 times larger than the current without radiation. The increase of the radiation dose rate causes an increase in the prebreakdown current. Breakdown occurred at lower voltages (205 V) in a γ radiation field. During the transition between nonconducting and conducting regime, the current increase is not as sharp as compared to the breakdown without irradiation.

Single electrons in atomic orbitals have low effective photoionization cross sections due to the small wavelength of high energy γ photons that cause ionization through the Compton effect [21].

The GFSA resistance versus applied voltage is shown in **Figure 7A** and **B**, without radiation and in $\text{Co } \gamma$ field, respectively. From the volt-ampere curve, the volt-ohm characteristic can be easily determined. Formula-defining relationship between resistance and voltage is obtained by linear regression, using least-square minimal error method. The following conclusions are made:

1. GFSA resistance shows linear increase with the applied voltage in the pre-breakdown regime. Increase is more prominent for type A commercial components than type B. Abrupt decrease of the resistance is observed as voltage reaches breakdown level.
2. Resistance also exhibits linear increase with the applied voltage in a γ radiation field but has one order of magnitude lower values than in operation without radiation. A slight decrease of the resistance is observed at voltage values near breakdown voltage; at breakdown voltage the decrease is pronounced.

The main conclusions of the experiment are:

1. In a γ radiation field, breakdown occurred at lower voltages (205 V). The values of breakdown voltage for two types of commercial GFSA have been determined in the presence of γ radiation and without radiation.
2. Prior to breakdown, the current had constant values, of the order of 0.1 nA. When voltage reached breakdown level, an abrupt increase of current was observed, current values reaching μA level.

3. In the prebreakdown regime, GFSA resistance increased linearly with the applied voltage. When the voltage reached breakdown level, an abrupt decrease of the resistance was observed.
4. γ radiation shows significant influence on GFSA performance. In prebreakdown regime, the current had one order of larger magnitude values than without radiation.
5. In a γ radiation field, resistance also showed a linear increase with the applied voltage, but one order of magnitude was lower than values without radiation.
6. All observed effects of γ radiation on GFSA commercial components had reversible character. Shortly after exposure (in a matter of hours), GFSA characteristics were the same as before irradiation.

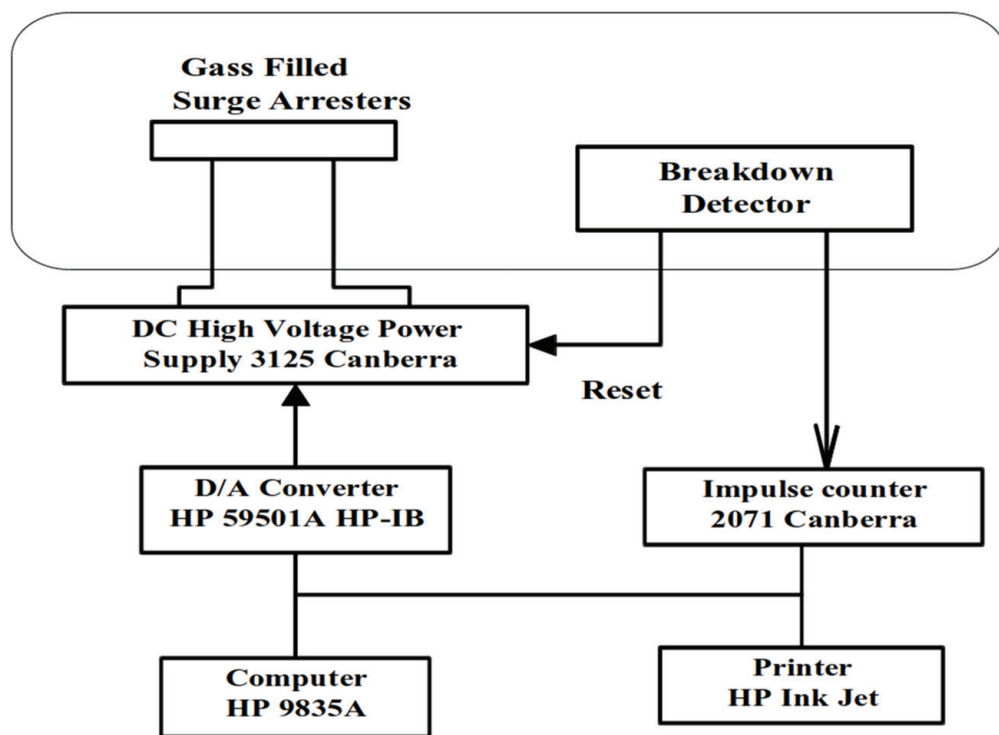


Figure 5. Scheme of the test cycle for investigating the radioactive resistance of GFSA by a DC voltage.

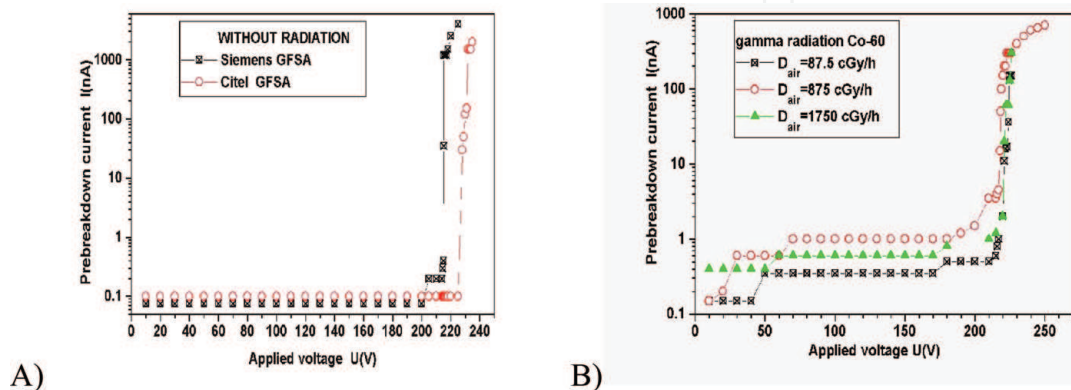


Figure 6. GFSA prebreakdown current without radiation (A) and under γ radiation (B) [9].

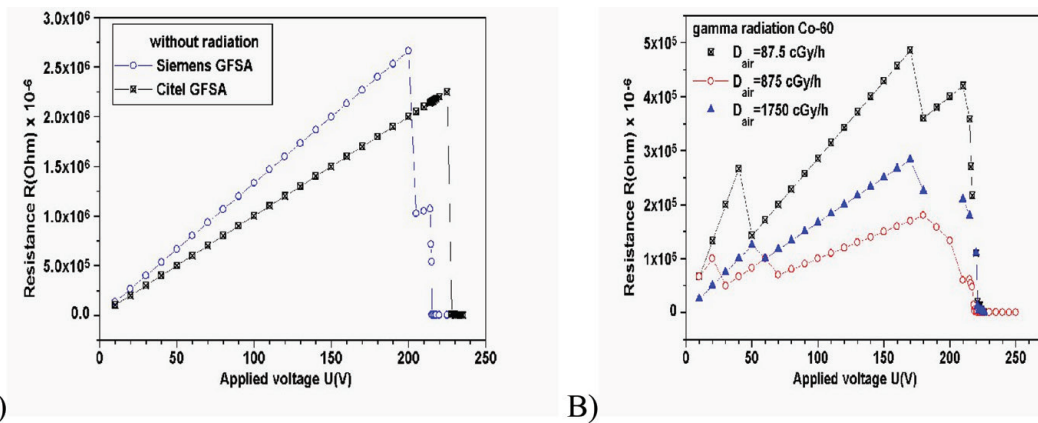


Figure 7. GFS resistance versus applied voltage without radiation (A) and under γ radiation (B) [9].

6. Testing the GFS model in γ radiation field

A model of GFS was constructed to allow the variation of relevant characteristics (chamber gas pressure and electrode materials), in order to test GFS performance in various operational regimes. The experiment was performed as follows: (1) GFS model was formed by choosing the appropriate material for the electrodes, placing the electrodes inside a gas-vacuum chamber, and setting the optimal electrode distance (**Figure 8A**); (2) the formed model (the gas tube) was connected to the gas-vacuum system with suitable valves, with a vacuum pump on one side and a steel gas supply cylinder on the other, and a pressure gauge; (3) the model was vacuumed by obtaining a stable pressure using valves leading to the vacuum pump and needle valves for grading the pressure; (4) the specific dose rate was set by appropriate positioning of the gas chamber relative to the source; (5) the electric circuit including the GFS was closed; (6) the electrodes were conditioned by being kept in discharge state for a while in order to attain stable working conditions and insure the repeatability of measured results; (7) the value of prebreakdown current was measured, as the applied voltage was gradually increasing in each of the experimental dose rates; and (8) resetting the experimental system at a different working point (electrode material, gas pressure, dose rate) and performing a new measurement procedure. The scheme of the experimental setup is presented in **Figure 8B**. Measuring equipment consisted of (1) gas-vacuum chamber, (2) pressure gauge Speedivac, (3) steel cylinder with pressurized Ar gas, (4) vacuum pump Edwards 5, (5) DC high voltage source, CANBERRA, (6) AVOMeter Iskra MI 7006, (7) digital multimeter LDM—852 A, (8) variable resistance MA 2110, and (9) coaxial cables and connectors.

Examination of the GFS was carried out in a gamma radiation field of ^{60}Co . The average energy of the applied gamma quanta was 1.25 MeV. The absorbed dose rate in air was, respectively, 96, 960, and 1920 cGy/h. The distance between the examined overvoltage components and the radioactive source was, respectively, 272, 86, and 60 cm. The distance between electrodes was 0.5 cm. All tests were carried out at pressures of 4666.27 Pa (35 Torr) and 2666.45 Pa (20 Torr), at room temperature of 20°C. The electrodes were made either of aluminum, steel, or brass.

Investigation of the dependence of the prebreakdown current on the applied voltage was performed under various experimental conditions: in the absence of radiation and in a gamma radiation field (for aluminum, steel, and brass electrodes), under two gas pressures. The results for DC current are presented in **Figures 9–11**, for aluminum, steel, and brass, respectively. In captions shown in these figures, current I_1 corresponds to the measurements without the radiation, current I_2 corresponds to the γ radiation absorbed dose rate of 0.96 Gy/h, current I_3

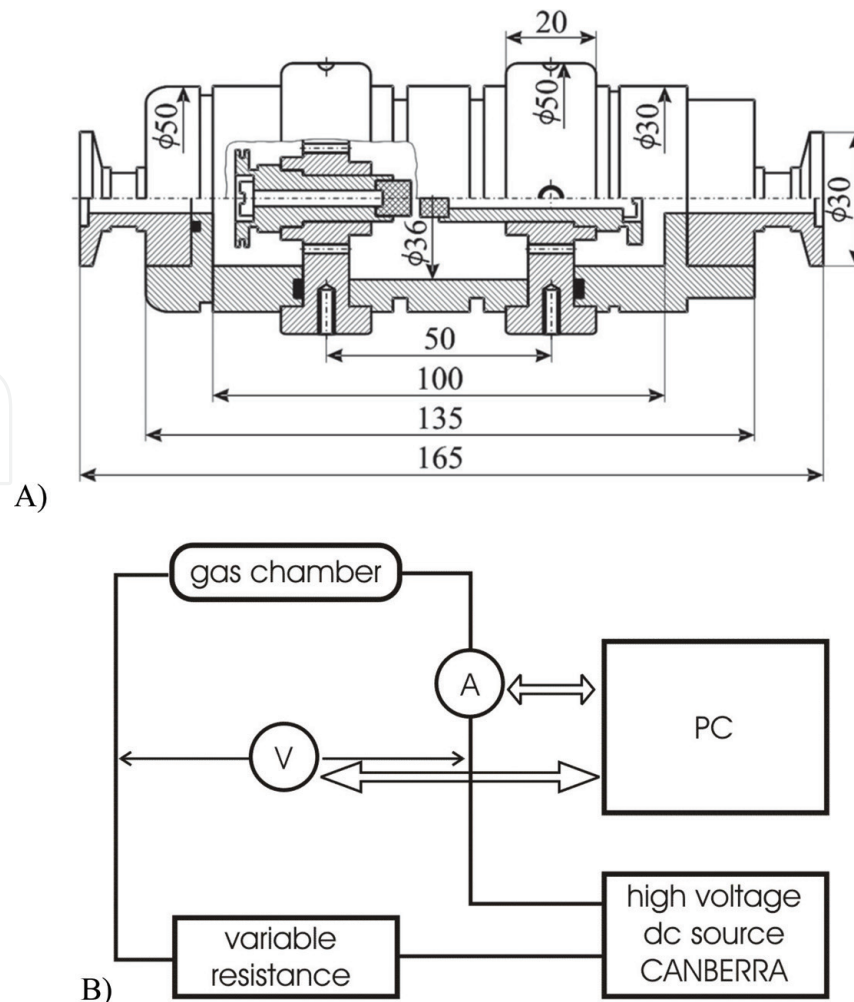


Figure 8. GFS model (dimensions in mm, A) [23] and the scheme of the test cycle (B).

corresponds to the γ radiation absorbed dose rate of 9.6 Gy/h, and current I_4 corresponds to the γ radiation absorbed dose rate of 19.2 Gy/h.

Gamma radiation has a strong influence on the prebreakdown current in GFS, as can be deduced from the presented graphs. Prebreakdown current is constant and independent of the applied voltage up to the value of the breakdown voltage in the absence of radiation. When ^{60}Co source is present, a steady rise of the prebreakdown current is observed, increasing with the increase of applied voltage. For all three-electrode materials, the rise of the prebreakdown current is more pronounced as the γ radiation dose increases, effective under both of the tested pressures. Breakdown voltage increased under higher gas pressure regime. The highest breakdown voltages were obtained using brass electrodes (up to 450 V), and the lowest were obtained using steel electrodes (from 320 to 350 V, depending on the radiation dose). Under lower pressure, for both steel and brass electrodes, higher radiation doses resulted in lower breakdown voltages, with the highest breakdown voltage measured when no radiation was applied. For aluminum, the highest breakdown voltage was obtained under highest radiation dose. The best performing GFS for DC current was the brass electrode under 20 Torr pressure.

Pulse shape (volt-second) characteristic is shown in **Figures 12–14**, respectively, for aluminum, steel, and brass electrodes. Experimental data indicates the following: γ radiation leads to a decrease in standard deviation and the narrowing of pulse shape characteristics of the arresters, which leads to an increase in the response speed. Because of that, we can conclude that γ radiation improves the performance of GFS. This phenomenon is most prominent in aluminum

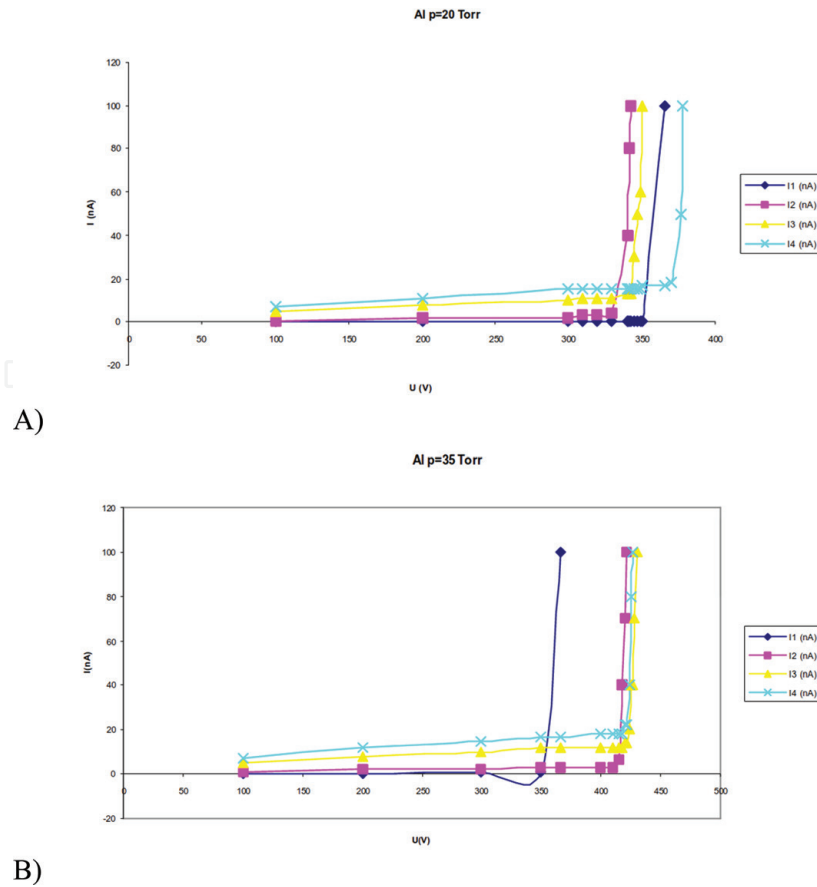


Figure 9. Prebreakdown current versus applied voltage in γ radiation field with aluminum electrodes under pressure of 20 Torr (A) and 35 Torr (B) [9].

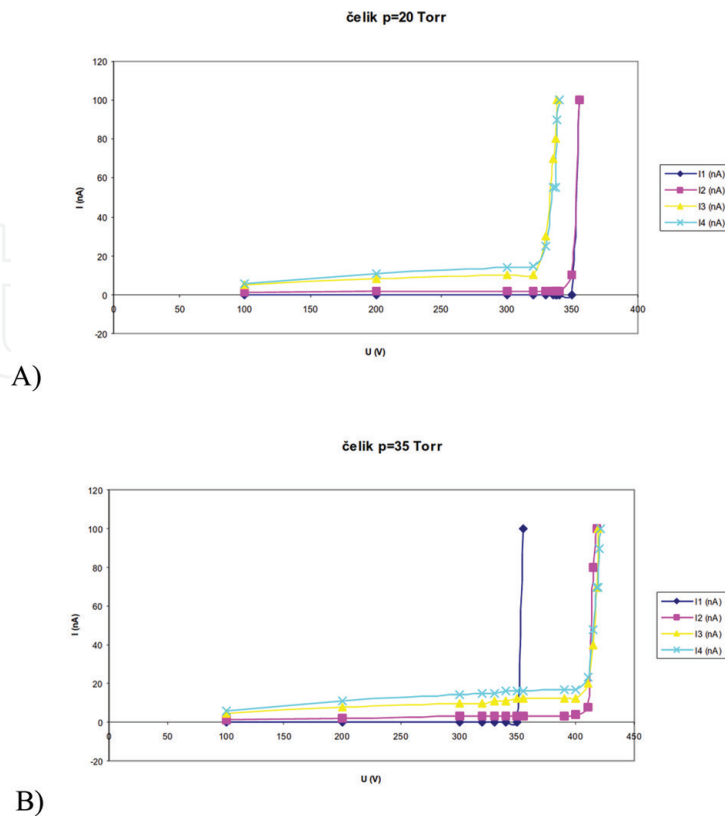


Figure 10. Prebreakdown current versus applied voltage in γ radiation field with steel electrodes under pressure of 20 Torr (A) and 35 Torr (B) [9].

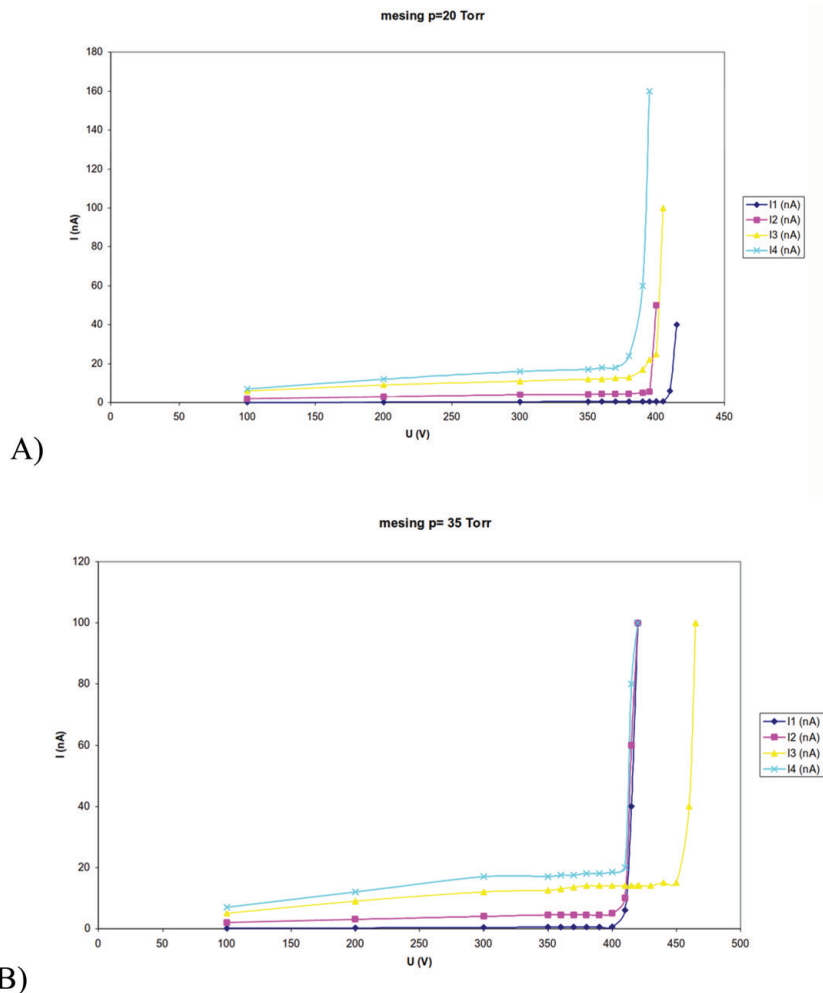


Figure 11. Prebreakdown current versus applied voltage in γ radiation field with brass electrodes under pressure of 20 Torr (A) and 35 Torr (B) [9].

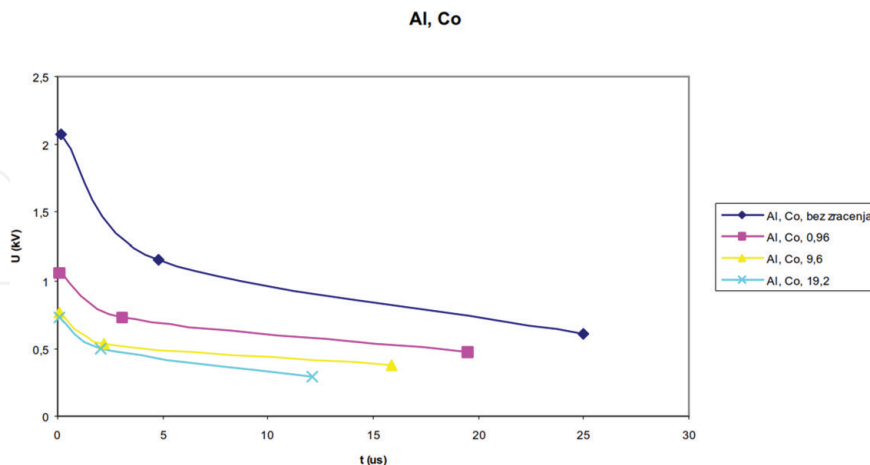


Figure 12. Pulse shape (volt-second) characteristic for aluminum electrodes in γ radiation field [9].

electrodes and least prominent in steel electrodes. Breakdown voltage deviation was least under the shortest pulses (1.2/50 μ s) and highest under the longest ones (100/700 ms). All the observed changes lasted only during γ radiation and reversed as soon as the radiation exposure ceased. The best pulse shape characteristic was obtained for aluminum electrodes, which had its performance improved under γ radiation [9].

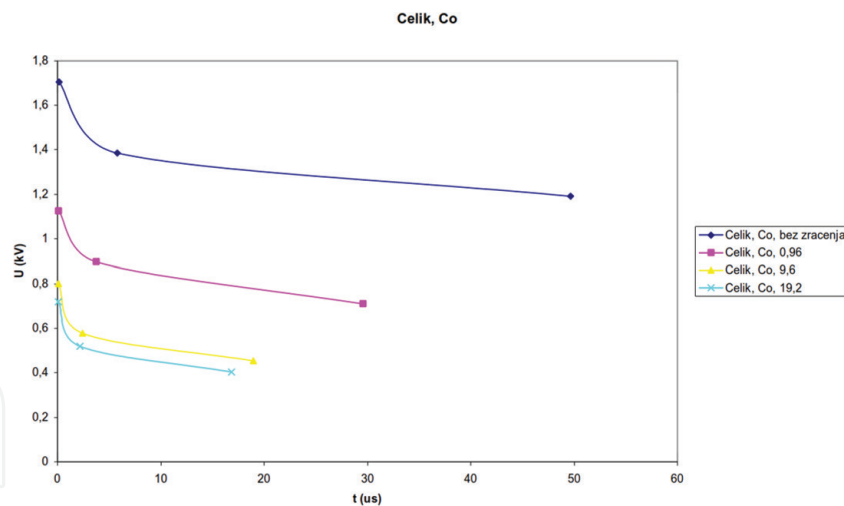


Figure 13. Pulse shape (volt-second) characteristic for steel electrodes in γ radiation field [9].

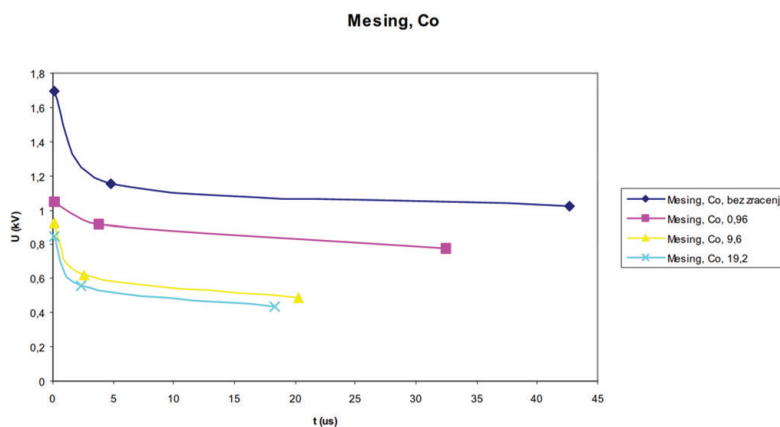


Figure 14. Pulse shape (volt-second) characteristic for brass electrodes in γ radiation field [9].

7. Conclusion

In this chapter, the influence of γ radiation on gas-filled surge arrester operation is discussed. An experimental model has been developed that allows easy modification of elements of the system and tests under different operational regimes. The experimental setup has also been used to test commercial GFSA components. An analytical method to describe GFSA pulse shape characteristics using area law has been established. These theoretical and empirical tools were used to measure and analyze the performance of different GFSA components exposed to combine $n + \gamma$ and pure γ radiation.

The experiments demonstrated that γ radiation improves the performance of GFSA. This effect was observed both in commercial components and the experimental model. The prebreakdown current had increased when GFSA were exposed to γ radiation. Beneficial effect of γ radiation on pulse shape characteristics was determined: due to the reduction of standard deviation, response time of GFSA was improved. These effects were consistent under different insulating gas pressure regimes. Among the metals tested as electrode materials using the model, brass was the best performing one. The effects of γ radiation were lasting only as long as the components were exposed. The performance of GFSA under γ radiation makes them suitable for overvoltage protection of electronic circuitry constantly or occasionally exposed to that type of radiation.

Acknowledgements

The authors thank the Ministry of Education, Science and Technological Advancement, Republic of Serbia, for supporting the research through projects no. 171007 and 43009.

Conflict of interest

The authors declare no conflict of interest.

Author details

Luka Rubinjoni¹, Katarina Karadžić² and Boris Lončar^{2*}

¹ Faculty of Technology and Metallurgy, Innovation Center, University of Belgrade, Serbia

² Faculty of Technology and Metallurgy, University of Belgrade, Serbia

*Address all correspondence to: bloncar@tmf.bg.ac.rs

IntechOpen

© 2019 The Author(s). Licensee IntechOpen. This chapter is distributed under the terms of the Creative Commons Attribution License (<http://creativecommons.org/licenses/by/3.0>), which permits unrestricted use, distribution, and reproduction in any medium, provided the original work is properly cited. 

References

- [1] Loncar B, Osmokrovic P, Stankovic S. Temperature stability of components for overvoltage protection of low-voltage systems. *IEEE Transactions on Plasma Science*. 2002;**30**(5):1881-1885
- [2] Osmokrovic P, Loncar B, Stankovic S, Vasic A. Aging of the over-voltage protection elements caused by over-voltages. *Microelectronics Reliability*. 2002;**42**(12):1959-1966
- [3] Osmokrovic P, Loncar B, Sasic R. Influence of the electrode parameters on pulse shape characteristic of gas-filled surge arresters at small pressure and inter-electrode gap values. *IEEE Transactions on Plasma Science*. 2005;**33**(5):1729-1735
- [4] Osmokrovic P, Stojanovic M, Loncar B, Kartalovic N, Krivokapic I. Radioactive resistance of elements for over-voltage protection of low-voltage systems. *Nuclear Instruments and Methods in Physics Research Section B: Beam Interactions with Materials and Atoms*. 1998;**140**(1-2):143-151
- [5] Markov Z. The comparison of modern over-voltage protection components. *Electrotechnics*. 1987;**10**(1):961-963
- [6] Loncar B, Osmokrovic P, Stankovic S, Filipovic D. Investigation the optimal method for improvement the protective characteristics of gas filled surge arresters-W/O the built in radioactive sources. In: *Pulsed Power Plasma Science 2001 "PPPS-2001"*, vol. 1. Digest of Technical Papers; 17 June 2001. IEEE. pp. 475-478
- [7] Loncar B, Osmokrovic P, Stankovic S. Radioactive reliability of gas filled surge arresters. *IEEE Transactions on Nuclear Science*. 2003;**50**(5):1725-1731
- [8] Loncar B, Osmokrovic P, Stankovic S, Sasic R. Influence of electrode material on gas-filled surge arresters characteristics in γ and X radiation field. *Journal of Optoelectronics and Advanced Materials*. 2006;**8**(2):863-866
- [9] Lončar B. Radijaciona otpornost memorijskih I prenaponskih zaštitnih komponenata. Beograd: Zadužbina Andrejević; 2006. 82 p
- [10] Loncar B, Osmokrovic P, Vasic A, Stankovic S. Influence of gamma and X radiation on gas-filled surge arrester characteristics. *IEEE Transactions on Plasma Science*. 2006;**34**(4):1561-1565
- [11] Osmokrovic P, Krivokapic I, Matijasevic D, Kartalovic N. Stability of the gas filled surge arresters characteristics under service conditions. *IEEE Transactions on Power Delivery*. 1996;**11**(1):260-266
- [12] Pejovic MM, Ristic GS, Karamarkovic JP. Electrical breakdown in low pressure gases. *Journal of Physics D: Applied Physics*. 2002;**35**(10):R91
- [13] Osmokrovic P. Mechanism of electrical breakdown of gases at very low pressure and interelectrode gap values. *IEEE Transactions on Plasma Science*. 1993;**21**(6):645-653
- [14] Loncar B, Novakovic D, Matijasevic D, Osmokrovic P. The influence of radioactive filling on efficient of gas filled surge arresters of small values of pd product. In: *Proceedings of XLIV Conference on Society for Electronics, Telecommunications, Computers, Automatic Control and Nuclear Engineering*. Belgrade, Serbia; 2000. Vol. 4. pp. 129-132
- [15] Matijasevic D, Loncar B, Krivokapic I, Novakovic D. Improvement of the protective characteristics of gas filled surge arresters using hollow cathode method. In: *Proceedings of XLII Conference on Yugoslav Society for*

Electronics, Telecommunications,
Computers, Automatic Control and
Nuclear Engineering. Belgrade, Serbia;
1998. Vol. 4. pp. 229-232

[16] Loncar B, Osmokrovic P, Stankovic
S, Vasic A. Static and dynamic
radioactive resistance of gas filled surge
arresters. In: Proceedings of 14th IEEE
Pulsed Power Conference; 15-18 June
2003; Dallas, United States: IEEE; 2003

[17] Djogo G, Osmokrovic P.
Statistical properties of electrical
breakdown in vacuum. IEEE
Transactions on Electrical Insulation.
1989;24(6):949-953

[18] Osmokrovic P, Krivokapic I,
Krstic S. Mechanism of electrical
breakdown left of Paschen minimum.
IEEE Transactions on Dielectrics and
Electrical Insulation. 1994;1(1):77-81

[19] ISO I, OIML B. Guide to the
Expression of Uncertainty in
Measurement. Geneva, Switzerland; 1995

[20] International Organization
for Standardization. Neutron
Reference Radiations for Calibrating
Neutron-Measuring Devices Used
for Radiation Protection Purposes
and For Determining Their Response
as a Function of Neutron Energy.
International Organization for
Standardization; 1989

[21] Messenger G, Ash M. The Effects
of Radiation on Electronic Systems.
New York: Van Nostrand Reinhold; 1992

[22] Rizk FA, Eteiba MB. Impulse
breakdown voltage-time curves of SF₆
and SF₆-N₂ coaxial-cylinder gaps. IEEE
Transactions on Power Apparatus and
Systems. 1982;(12):4460-4471

[23] Stanković K, Brajović D, Alimpijević
M, Lončar B. Long-term deconditioning
of gas-filled surge arresters. Radiation
Effects and Defects in Solids.
2016;171(7-8):678-691